Sculpturing Effect of Chloride Ions in Shape Transformation from Triangular to Discal Silver Nanoplates

Jing An, Bin Tang, Xianliang Zheng, Ji Zhou, Fengxia Dong, Shuping Xu, Ye Wang, Bing Zhao, and Weiqing Xu*

State Key Laboratory of Supramolecular Structure and Materials, Jilin University, Changchun 130012, P. R. China

Received: March 28, 2008; Revised Manuscript Received: August 4, 2008

The sculpturing effect of chloride ions on the shape transformation of silver nanoparticles is presented. UV−vis spectroscopy and transmission electron microscopy (TEM) were used to monitor the evolution of silver nanoplates. Cl^- can etch the corners and side faces of the silver nanoprism, and the resulting nanoparticles are disk-like in shape. The dissolved silver atoms would aggregate to form small silver clusters, which were stabilized by the Cl^- and citrate ions. The facet-selective etching effect of Cl^- is mainly attributed to the surface energy difference of each face of the nanoplate. The thickness of the nanodisk increased during the etching process because of the redeposition of sliver clusters on the {111} planes. The prepared nanodisk also gave rise to high SERS intensity of the probing molecule.

1. Introduction

Noble metal nanoparticles are of great interest in recent years because of their unique chemical and physical properties,[1] and the wide range of potential applications including surface plasmon resonance (SPR),[2] surface-enhanced Raman scattering (SERS),[3] biosensing,[4] and optoelectronic devices.[5] The properties of noble metals in the nanoscale can be finely tuned by adjusting their shapes, sizes, and modifications on their surfaces. Silver nanoparticles are ideal building blocks in the design of plasmonic materials[6] and nanodevices.[5] As a result, great efforts have been made to control the size and shape of silver nanoparticles. A mass of approaches and methods, such as photochemical[7] and thermochemistry[8] methods, have been developed and employed in the synthesis of silver nanoparticles. So far, silver nanoparticles in the shape of wire,[9] belt,[8a] bar and rice,[10] prism,[7a,b,11] disk,[12] and cube,[13] and so forth have been obtained.

Recently, there were some reports introducing several etching means to adjust the shape of silver nanoparticles via the shape transformation process. It has been reported that the truncation at the corners of silver nanostructures might be achieved by heating.[14] In addition to thermal aging, Xia et al.[15] have reported a simple method to obtain Au−Ag alloy nanocages containing hollow interiors and controllable pores at all corners through the galvanic replacement reaction between Ag nanocubes and aqueous $HAuCl_4$. Su et al.[16] reported that the assembled nanoprisms can be transformed into disk-like shape by immersing the assembled substrate in buffer solutions of different pH value, in which the shape transformation might be due to the etching effect of H^+ derived from the buffer solution. The significant roles of the inorganic species in controlling the shape of nanoparticles have been described. Xia and co-workers[17] have reported that the Cl^-/O_2 pair can oxidatively etch twinned nanoseeds. Such an etching process resulted in high-yield single-crystal nanoseeds and the produced nanoparticles were truncated nanocubes and a tetrahedron. However, the effect of chloride ions in the shape control of nanoparticles was mostly investigated and employed in the seed-mediated growth process. The role of chloride ions in shape-controlled synthesis still needs further research. In addition, a systematic study of the effect of chloride ions on silver nanoparticles is important for application of silver nanoparticles in variable fields. For example, the influence of chloride ions on SERS activity of silver nanoparticles has been investigated. The high increase of SERS signals have been reported upon the addition of halide ions to silver colloids,[18] whereas the decrease of SERS activity resulting from the addition of halide ions was also reported.[19] The influence of the addition of chloride ions on silver nanoparticle should be further investigated, which is favorable for exploring the potential application of silver nanoparticles in chemical and biological sensing.

Herein, we developed a simple and convenient method to transform silver nanoprisms into nanodisks by adding the chloride ions into the silver colloid. The shape transformation of the nanoprism might be due to the facet selective etching effect of chloride ions at their corners and the side facets. The dissociated silver atoms would aggregate and appear in the form of clusters in sizes below 3 nm, which can be found in the colloidal system after the sculpturing process. Moreover, some of the dissociated silver atoms might redeposit on the flat facets and thus increase the thickness of the nanoplates. The role of the chloride ion in our case is quite different from that reported previously, which might be able to provide a new and simple method to adjust the shape and size of nanoparticles. The discussion on the role of chloride ions in shape transformation would redound to further understanding the mechanism of the chloride ion etching effect. The obtained nanodisk showed higher SERS activity than the original nanoprism.

2. Experimental Section

2.1. Materials. $AgNO_3$ (99.8%) was obtained from Shanghai reagent NO.1 Plant. $NaBH_4$ (96.0%) was obtained from Sinopharm Chemical Reagent Co., Ltd. Trisodium citrate (99.0%) and potassium chloride (99.99%) were purchased from Beijing Chemical Plant. Potassium chloride was of high purity grade, and other chemicals were analytic grade reagents. All chemicals were used without further purification.

* To whom correspondence should be addressed: Tel: +86-431-85159383. Fax: +86-431-85193421. E-mail: xuwq@jlu.edu.cn.

10.1021/jp802694p CCC: $40.75
Published on Web 09/10/2008

TABLE 1: Evolutions of the Silver Colloid by Increasing the M_{Cl^-}/M_{Ag} in the Range of 0−80

	trials										
M_{Cl^-}/M_{Ag}	0:1	6:1	8:1	10:1	12:1	15:1	20:1	30:1	45:1	60:1	80:1
UV−vis curve	(0)	(1)	(2)	(3)	(4)	(5)	(6)	(7)	(8)	(9)	(10)
stability	colloid	colloid					colloid				aggregation
variety of color		blue, a little darker					purple−red				colorless

2.2. Instrumentation. A 70-W sodium lamp (Shanghai Yaming Co., Ltd.) was used as the light source for the photochemical preparation of silver prisms. UV−vis spectra were recorded by a Shimadzu UV-3100 spectrophotometer. Transmission electron microscope (TEM) images were measured with a Hitachi H-8100 IV operating at 200 kV. Samples for TEM analysis were prepared by dripping a drop of silver nanoparticle colloid onto the carbon-coated copper grids and drying in air at room temperature. High-resolution TEM (HRTEM) images were measured with a JEOL 3010 high resolution transmission electron microscope operating at 300 kV. Specimens for HRTEM were prepared by depositing a drop of colloidal solution onto holey carbon-coated Cu grids. Analysis of X-ray photoelectron spectroscopy (XPS) was performed on ESCLAB MKII using Al as the excitation source. The specimens for XPS were prepared by assembling original silver nanoprisms on the glass slides, and nanodisks were obtained by in situ shape transformation. Raman spectra excited at 514.5 nm were obtained with a Renishaw Raman system model 1000 spectrometer. The 514.5 nm radiation from an air-cooled argon ion laser was used as the excitation source, and the power of the laser was 16 mW. Raman spectra excited at 785 nm were obtained with a BAC100-785Q Raman probe and a BTC112E CCD spectrometer. The 785 nm excitation line was from the BRM-785 laser, and the laser power was 117 mW. At the excitation wavelength of 514.5 or 785 nm, data acquisition involved a 10 s accumulation for the detection. 4-Mpy as probe molecules were absorbed on the assembled original silver nanoprisms and nanodisks that were in situ transformed from the nanoprisms. The in situ transformed nanodisks were obtained by immersing the assembled original nanoprisms in KCl solution (10 mM) for a short time. Powder X-ray diffraction (XRD) data were collected using a Rigaku D/Max 2550 V/PC X-ray diffractometer with Cu Kα radiation ($\lambda = 1.5418$ Å) at 40 kV and 200 mA at room temperature.

2.3. Preparation of Silver Nanoprisms. Silver nanoprisms were synthesized via a photoinduced growth process as described previously.[20] Briefly, silver nanoseeds were prepared by dropwise addition of $NaBH_4$ solution (8.0 mM, 1.0 mL) to an aqueous solution of $AgNO_3$ (0.1 mM, 100 mL) in the presence of trisodium citrate (1.5 mM) under vigorous stirring. The yellow colloid of the silver nanoseeds was then irradiated by a conventional 70-W sodium lamp. The color of the colloid gradually turned to green and became blue eventually. The obtained nanoparticles were triangular nanoplates, with an edge length of 70.0 nm and a thickness of 10.2 nm.

2.4. Sculpturing Process of Chloride Ion on Silver Nanoprisms. A 5 mL KCl solution was added into 10 mL of nanoprism colloid (0.1 mM; refer to the initial concentration of silver ions) with the molar ratio (M_{Cl^-}/M_{Ag}) in the range of 0−80 under vigorous stirring. Significant change in color was observed as the molar ratio increased (listed in Table 1). When adjusting the molar ratio to a certain range, the colloid changed into purple−red in color.

3. Results and Discussion

Significant changes in color of the nanoprism colloid were observed as different amounts of KCl solution were added as listed in Table 1, and the corresponding photograph of the obtained solution with various chloride ion concentrations is shown as inset of Figure 1. When low concentration of KCl solution was added, making M_{Cl^-}/M_{Ag} in the range of 0−8, the color of the colloid was darkened a little. As M_{Cl^-}/M_{Ag} increased to the range of 10−60, remarkable change in the color of the colloid could be observed. The final colloid solution appeared purple−red in color. However, as M_{Cl^-}/M_{Ag} was higher than 80, nanoparticles in the colloid would get aggregated and precipitated. As a result, the colloid was colorless. The evolution processes were monitored through UV−vis spectroscopy (Figure 1) and TEM characterization (shown in Figure 2). The role of Cl^- in the evolution process was investigated as well.

As shown in Figure 1, curve (0) is the spectrum of the original silver nanoprism colloid, which is blue in color. Three plasmon resonance bands can be observed in curve (0), which are centered at 331 (weak), 515 (medium), and 702 (strong) nm, and are assigned to out-of-plane quadrupole, in-plane quadrupole, and in-plane dipole plasmon resonance modes of silver nanoprisms, respectively.[7a,b,21] Curves (1) and (2) show the final spectra of the colloid when M_{Cl^-}/M_{Ag} was 6 and 8, respectively. As can be seen, the main bands of the nanoparticles in curves (1) and (2) blue-shifted a little as compared to the original nanoprism, without changing the profile of the spectra. The slight blue shift might be due to a mild truncation at the sharp corners of the nanoprism. The decrease in band intensity might be caused by the dilution with the addition of KCl solution. As M_{Cl^-}/M_{Ag} increased to the range of 10−60, a big blue shift of the dipole plasmon resonance band can be observed as shown in curves (3)−(9). The remarkable blue shift from 702 nm to 480 nm might indicate a serious truncation at the corners of the nanoprism. As a result, the morphology of the nanoparticles might be changed and transformed into other shapes. However, the final band positions and profiles of the spectra were almost the same as shown in curves (3)−(9), indicating that the increase in the amount of chloride ions in this range did not influence the final state of the colloidal system. The sudden change in the UV−vis spectra occurred when M_{Cl^-}/M_{Ag} changed from 8

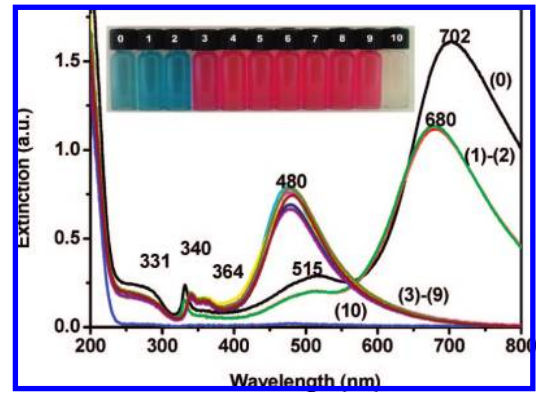

Figure 1. UV−vis spectra of silver colloid obtained with different values of M_{Cl^-}/M_{Ag}. The values of M_{Cl^-}/M_{Ag} in spectra (0)−(10) correspond to that shown in Table 1. Insert: Photograph of the solution with various chloride ions concentration 0−10 corresponding to the molar ratios of Cl^- to Ag^+ in Table 1.

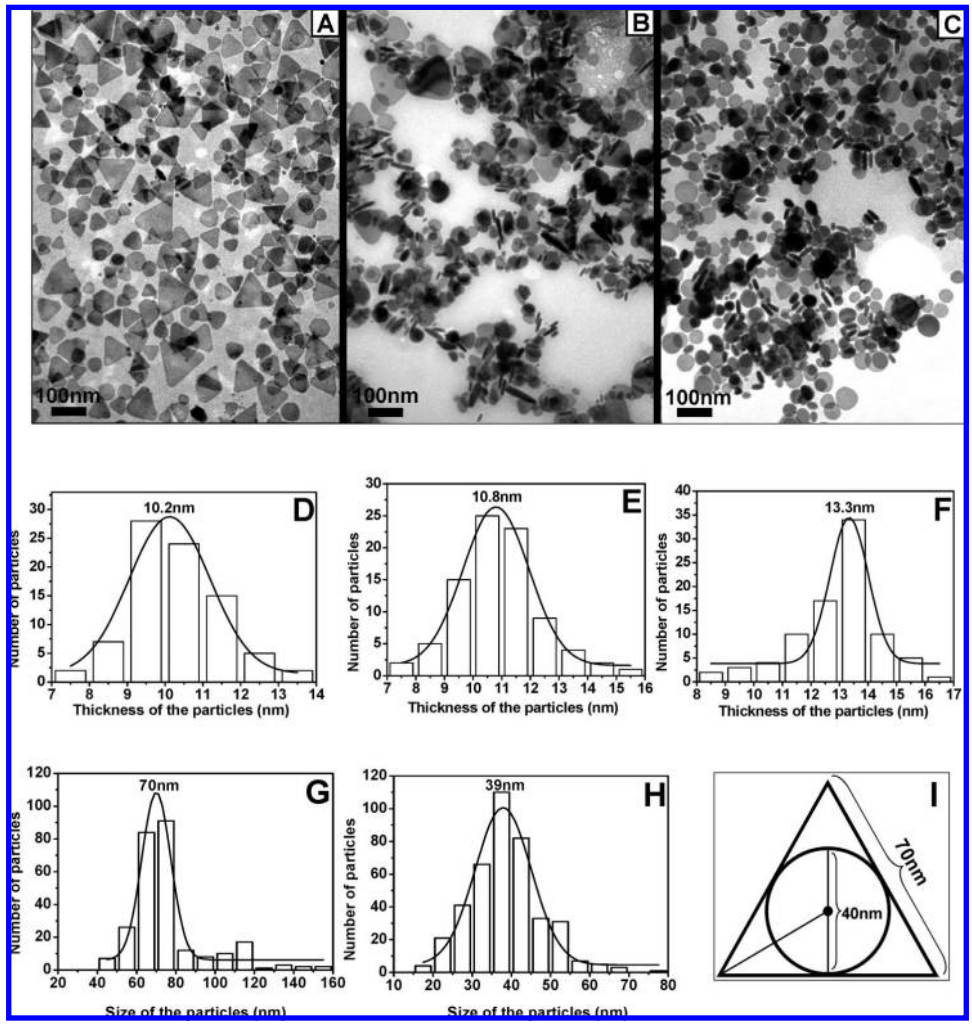

Figure 2. TEM images of silver nanoparticles obtained with the values of M_{Cl^-}/M_{Ag} equal to 0 (A), 8 (B), and 15 (C), respectively. Histograms of the thickness of the obtained silver nanoparticles (D, E, and F). D, E, and F correspond to the images of A, B, and C, respectively. Histograms of the edge lengths of silver nanoprisms (G) and the diameters of silver nanodisks (H), and the geometrical illumination (I) of the relationship between the nanostructures before and after the shape transformation process.

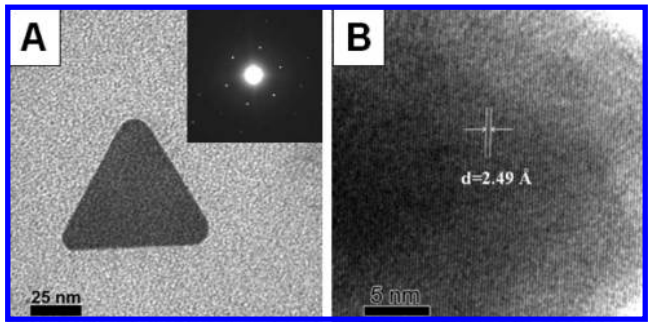

Figure 3. (A) TEM image of an individual silver nanoprism and its corresponding electron diffraction pattern (shown in the inset picture). The electron diffraction pattern was obtained by directing the electron beam perpendicular to the flat face of the nanoplate. (B) HRTEM image of silver nanoprism by directing the electron beam perpendicular to the flat face.

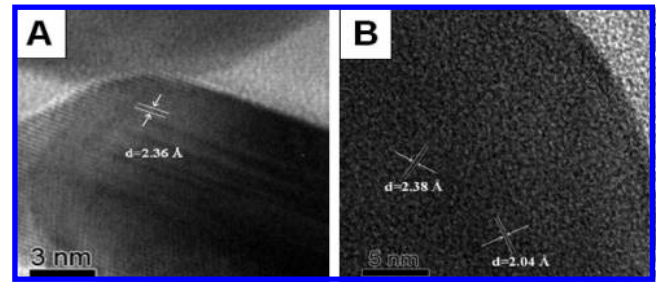

Figure 4. HRTEM images of the nanodisk by directing the electron beam perpendicular to its side face (A) and its flat face (B).

to 10. The sudden shift of UV−vis spectra implied that the colloid changed from one state into another. In both states, the configurations of the nanoparticles were stable. When M_{Cl^-}/M_{Ag} was as low as 8, the addition of chloride ions would disturb the colloidal system slightly, and the shape and size of the nanoparticles might change a little, which could caused a slight blue shift of the main band of the silver colloid. When M_{Cl^-}/M_{Ag} was as much as 10, the nanoparticles in the colloidal system could not hold their original morphology. As a result, the colloidal system changed from one state into another, which caused an obvious blue shift in the UV−vis spectrum.

To investigate the process described above, the TEM images of the original colloid and the final colloids obtained by the chloride ion etching process were taken, as shown in Figure 2. Image (A) shows the TEM image of the original colloid, in which nanoprisms with sharp corners can be observed. As a slight amount of KCl solution was added, the nanoprisms in the colloid got rounded a little at the corners as shown in image (B). The slight truncation at the corners of the nanoprisms might be able to cause a slight blue shift of the dipole resonance band

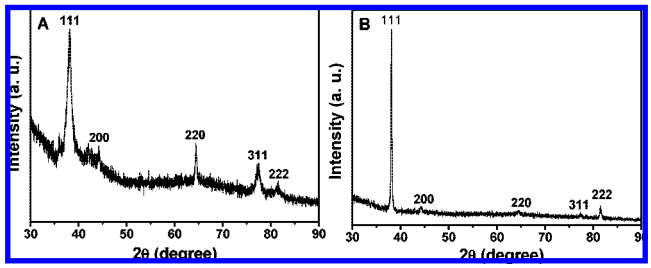

Figure 5. XRD patterns of the silver nanoprism (A) and silver nanodisk (B).

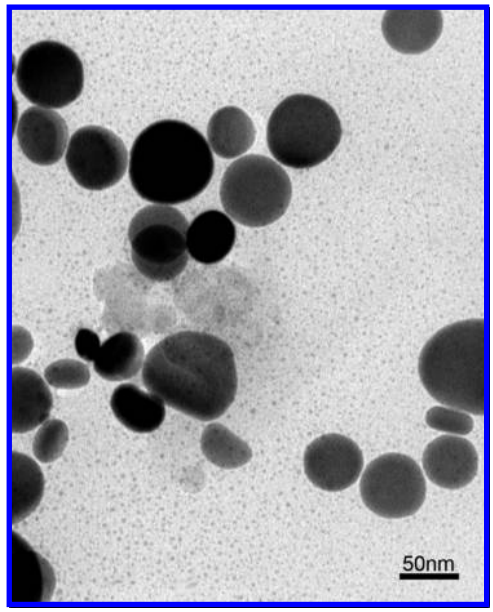

Figure 6. TEM image of silver clusters dispersed in the colloid system.

as shown in curves (1) and (2). Image (C) shows the nanoparticles obtained by increasing M_{Cl^-}/M_{Ag} to 10−60, in which the discal nanoplates are the main products in the colloid. It can be seen that the obtained nanodisks might be formed by a serious truncation at the corners of nanoprisms. The thickness of nanoplates can be measured because some of the nanoparticles stack and stand on the TEM grids. Through the analyses of TEM images, the thicknesses of nanoparticles in images (A), (B), and (C) were measured. The average thickness of nanoparticles in image (D) is 10.2 nm, and that in image (E) is 10.8 nm and 13.3 nm for nanoparticles in image (F). We found that the thickness of the nanoparticles increased as the truncation degree at the corner of the nanoprism increased, which resulted from the increase of M_{Cl^-}/M_{Ag}. The evolutions in the truncation degree at the corner and the changes in thickness should be reasonable to explain that the blue shift occurred in the UV−vis spectrum as described above.

It has been reported by Xia et al.[13,17] that the Cl^-/O_2 pair can selectively etch the twin crystal in the polyol synthesis of unique silver nanocubes and tetrahedron. In order to examine whether the oxygen dissolved in the solution assists the chloride ion in etching the nanoplates, we removed the dissolved oxygen by bubbling nitrogen in both silver colloid and KCl solutions, before adding the KCl solution. However, the observed phenomenon was the same as that without removing the oxygen, which implied that oxygen was not necessary in shape transformation. Thus, the role of the chloride ion here might be different from that discussed in Xia's work.

Both UV−vis spectroscopic and TEM characterizations confirmed that the sculpturing effect of the chloride ions can facilely transform the shape of the silver nanoparticles, from triangular plates with sharp corners into disk-like plates in our case. The average edge length of the nanoprism was measured to be about 70.0 nm (Figure 2G), and the average diameter of the obtained nanodisk was about 39.0 nm (Figure 2H). It is interesting that the inscribed circle of the nanoprism is about 40.4 nm in diameter, which is consistent with that of the obtained nanodisk (the geometrical illuminate shown in Figure 2I), indicating that the nanodisks might derive from nanoprisms through the truncation of silver atoms at the corners.

Figure 3A shows the electron diffraction pattern taken from an individual nanoprism by directing the electron beam perpendicular to its flat face. The electron diffraction pattern indicates that the nanoprism is a single crystal. The hexagonal symmetry of the patterned spots implies that the flat face of the nanoprism is {111} plane. Furthermore, Figure 3B shows the HRTEM images of the nanoprism recorded perpendicular to its flat face. The fringes of the silver nanoprism are separated by 2.49 Å, which can be ascribed to the (1/3){422} reflection that is generally forbidden for an fcc lattice.[7a,b,8a,11e,12a] It has been previously reported that the basal plane of the silver nanoprism is {111} plane and that the side plane is {110} plane.[7b] Figure 4 shows the HRTEM images of the nanodisk by directing the electron perpendicular to its side face (A) and the flat face (B). The lattice spacing of the side face is measured to be 2.36 Å, corresponding to the {111} plane of fcc silver metal, which implied that the flat planes did not change in the sculpturing process. Moreover, Figure 4B shows the lattice spacing of 2.04 Å ascribed to the {100} reflection and a lattice spacing with 2.38 Å attributed to the {111} reflection. To further identify the crystal structure of these two kinds of silver nanoplates, the XRD patterns are investigated and shown in the Figure 5. As can be seen in the XRD pattern, there are two strong peaks attributed to {111} and {220} peaks for triangular nanoplates, which implies that the triangular nanoplates are mainly bound by the {111} and {110} planes (Figure 5A). The basal planes are proved to be {111} facets by the HRTEM; therefore, the side faces are {110} plane, which are consistent with the result reported by Mirkin et al..[7b] In Figure 5B, only one strong peak indexed as the {111} peak for nanodisks is observed, and other peaks are very low in intensity, which implies that the {111} plane as the basal face is predominant and that the side faces may be a mixture of different crystal planes in the nanodisk.

How does the chloride ion affect the morphologic transformation of silver nanoprisms? On the one hand, on the basis of the Gibbs−Thomson effect, a convex surface has a higher surface energy than a flat surface. The convex surface of the nanoprism would be less stable in the present of chloride ions and might be able to explain the preferential etching of the corners in silver nanoprisms rather than other areas. In addition, the basal plane of the silver nanoprism is {111} plane and the side plane is {110} plane.[7b] The silver atoms at the corner areas and on the {110} facet have less coordination number than those on the {111} facet, which results in higher surface energy at the corner areas and the side facets of the nanoprism.[22] In this case, the atoms at the corner areas and on the side facets can be readily broken away from the entire nanostructure on the addition of Cl^-. On the other hand, there are also some chemical factors that might influence the facet-selecting etching of chloride ion. As is well known, Cl^- can serve as a precipitant of Ag^+ at a low concentration and a complexant at a high concentration.

SCHEME 1: Process for Chloride Affecting a Silver Nanoprism

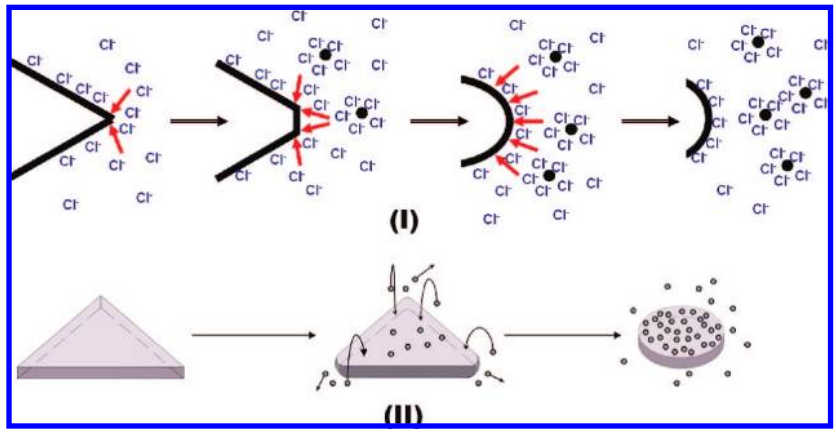

The chloride ions can coordinate with the active silver atoms and dissociate them from the nanostructure. Moreover, the vertex areas of the nanoprism are less stabilized by the citrate ions. As a result, silver atoms at these areas can be readily attacked by Cl^- and separated from the original nanostructure. Thus, the vertex areas were selectively etched during the sculpturing process. In contrast, the {111} facets are capped by more citrate, which has been reported previously,[11c,20] preventing them from the attack of Cl^-. It is probable that a combination of multifold driving forces produce the selective sculpturing of the silver nanoprisms. However, it is suggested that the difference of surface energy between the corner and {110} facet and {111} facet is the pivotal driving force determining the shape transformation from prism to disk in the etching of chloride ions.[23]

A lot of super-small nanoparticles were found in the TEM images (Figure 6). The size of super-small silver nanoparticles was below 3 nm, and we considered them as silver clusters. However, we did not observe any nanoclusters in the original nanoprism colloid. The silver clusters probably resulted from the aggregation of the dissociated silver atoms that were produced during the sculpturing process. The silver clusters were stable in the colloid, which might be electrostatically stabilized by the chloride ions adsorbed on their surface. Thus, the chloride ions also acted as the stabilizers in the sculpturing process. The stabilizing role of Cl^- has also been observed by Xia and other groups.[13,17] Why did the average thickness of nanoplates increase with the increase of molar ratio of Cl^-/Ag? It was probably because the dissociated silver atoms redeposited on the {111} plane. By calculating the volume of the obtained nanodisk (39 nm in diameter, 13 nm in thickness) and the original nanoprism

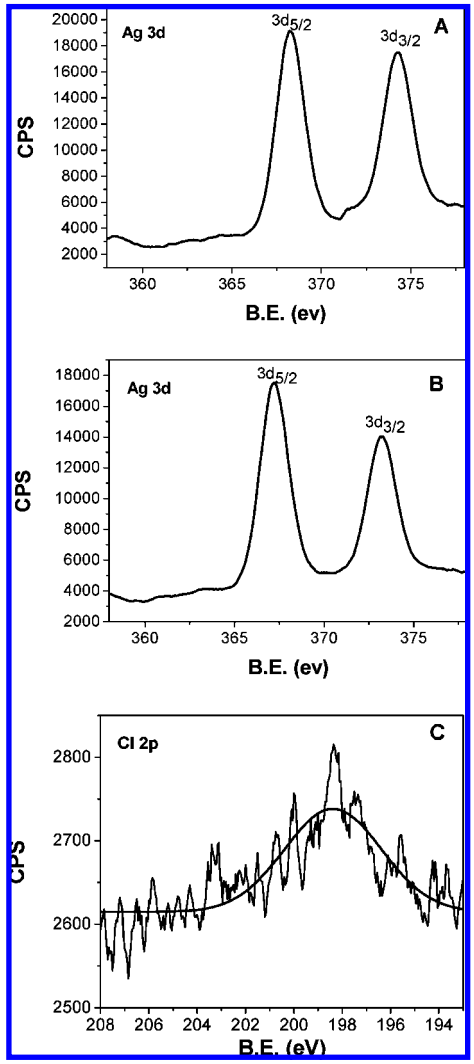

Figure 7. XPS of the assembled nanoprisms (A) and nanodisks (B, C) obtained by immersing the assembled nanoprisms in Cl^- solution (10 mM). (A) Ag 3d; (B) Ag 3d; (C) Cl 2p.

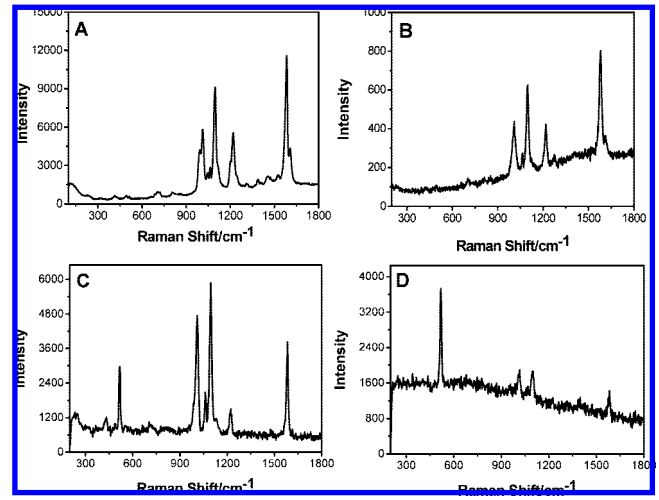

Figure 8. SERS spectra of 4-MPY obtained from substrates of silver nanodisks (A, C) and nanoprisms (B, D) by using two different excitation wavelengths. A and B: Excitation line $\lambda_0 = 514.5$ nm; laser power, 16 mW. C and D: Excitation line, $\lambda_0 = 785$ nm; laser power, 117 mW. The integration time is 10 s.

(70 nm in edge length, 10 nm in thickness), we found that the volume decreased a little for the nanodisk as compared to that of nanoprism, indicating that some of the dissociated silver atoms were not redeposited on the flat planes.

The proposed mechanism of the sculpturing process is depicted schematically in Scheme 1. The plausible procedure is listed as follows: first, chloride ions attack at the vertex areas of the prism and carve away the silver atoms from those places. Then, more silver atoms would be dissociated by Cl^- as more active areas were produced by the initial sculpturing process. Finally, the disks formed as the corners were completely dissolved. The silver atoms that dissociated from the nanostructures aggregated and formed sliver clusters, which might be stabilized by the chloride ions adsorbed on the outside. The Cl^- coated silver clusters might diffuse to and adsorb onto the {111} facets of the nanoplates and thus make the thickness of the nanoplates increase a little as compared to that of the the original ones. The redeposition process of the silver atoms on the flat plane is shown in Scheme 1 (II).

To further illustrate the shape transformation process, the XPS of both the nanoprism and nanodisk were detected, as shown in Figure 7. By comparing the XPS of both nanoplates, we found that the peaks of (Ag 3d) were essentially the same, except for the lower intensity of peak (Cl 2p) in XPS of nanodisks. The result indicates that a trace of Cl is present on the {111} facets of nanodisks, which is consistent with the mechanism proposed above. Although some questions still remain as to the mechanism of the shape transformation process, it is interesting that sculpturing with chloride may develop a novel route to fabricate nanoparticles with controllable shape.

Silver nanoparticles have shown wide applications in optics due to their inherent properties such as SPR.[24] Diversely shaped silver nanoparticles have been applied as the substrates to enhance the normal Raman signals of probing molecules.[25] Herein, the prepared silver nanoprisms and nanodisks were used as the SERS substrates, and 4-MPY was used as the probing molecule to investigate their SERS activities. Figure 8 show the SERS spectra of 4-MPY (1.0×10^{-4} M) adsorbed the on Ag nanodisk (curve A) and Ag nanoprism (curve B) with an excitation wavelength of 514.5 nm. Although both the silver nanodisk and nanoprism showed strong Raman signals of 4-MPY, the former substrate provided an order of magnitude higher signals than the latter one. We also introduced the 785-nm laser as the exciting light to investigate the SERS activities of these two substrates, as shown in Figure 8C and D. Curve C shows the SERS spectrum of 4-MPY (1.0×10^{-4} M) adsorbed on the silver nanodisk at an excitation wavelength of 785 nm, and curve D corresponds to that on the silver nanoprism. The peak center at 520 cm^{-1} in Figure 8C and D was Raman signals of the silicon slip used as the assembly substrate. Similar to the result detected by the 514.5-nm laser, the signals of 4-MPY on the nanodisk was an order of magnitude higher than that on the nanoprism. Under the excitation of the visible and near-infrared wavelengths, the nanodisk showed both higher SERS signals, which might be due to the existence of silver clusters in the colloid systems, and the adsorption of chloride ions on the surface of nanoparticles as well. Further studies on the activities of SERS of nanoprisms and nanodisks are in process.

4. Conclusions

In summary, we have demonstrated a new strategy for the high-yield, controllable synthesis of the silver nanoplates in disk-like shape. Chloride ion, the etching agent, can selectively sculpture the {110} facets of silver nanoprisms and transform their shapes into planar disk-like, as discussed in the present article. The mechanism of shape transformation of the silver nanoprism was proposed and discussed. The facet-selective etching of Cl^- is probably attributed to the difference in facet surface energies as well as the distinct stabilities of citrate ions on different faces. The role of Cl^- in the shape transformation process was also investigated, which may help us to further understand the pivotal effect of Cl^-. Moreover, we found that the as-prepared nanodisks showed higher SERS activity as compared to that of the original nanoprisms, which might be due to the existence of the silver cluster in the system of silver nanodisks. The sculpturing effect of Cl^- might provide an interesting way to tune the optical properties of nanoparticles. The sculpturing methodology may also be applied to metal nanoparticles in other shapes. We expect that many new shapes and sizes of nanoparticles will appear as this sculpturing effect is integrated into other strategies of nanoparticle synthesis.

Acknowledgment. This work was supported by the National Natural Science Foundation of China (NSFC20573041, 20773045, and 20627002).

References and Notes

(1) (a) Cao, Y. W.; Jin, R. C.; Mirkin, C. A. *Science* **2002**, *297*, 1536. (b) Wiley, B.; Im, S. H.; Li, Z. Y.; McLellan, J. M.; Siekkinen, A.; Xia, Y. *J. Phys. Chem. B* **2006**, *110*, 15666. (c) Wu, Y.; Messer, B.; Yang, P. *Adv. Mater.* **2001**, *13*, 1487. (d) Salzemann, C.; Lisiecki, I.; Brioude, A.; Urban, J.; Pileni, M.-P. *J. Phys. Chem. B* **2004**, *108*, 13242. (e) Wang, Z. L.; Ahmad, T. S.; El-Sayed, M. A. *Surf. Sci.* **1997**, *380*, 302.

(2) (a) Sherry, L. J.; Chang, S.-H.; Schatz, G. C.; Van Duyne, R. P.; Wiley, B. J.; Xia, Y. *Nano Lett.* **2005**, *5*, 2034. (b) Sherry, L. J.; Jin, R.; Mirkin, C. A.; Schatz, G. C.; Van Duyne, R. P. *Nano Lett.* **2006**, *6*, 2060.

(3) (a) Haynes, C. L.; Van Duyne, R. P. *J. Phys. Chem B* **2003**, *107*, 7426. (b) Michaels, A. M.; Nirmal, M.; Brus, L. E. *J. Am. Chem. Soc.* **1999**, *121*, 9932. (c) Zheng, X.; Guo, D.; Shao, Y.; Jia, S.; Xu, S.; Zhao, B.; Xu, W.; Corredor, C.; Lombardi, J. R. *Langmuir* **2008**, *24*, 4394. (d) Li, X.; Xu, W.; Zhang, J.; Jia, H.; Yang, B.; Zhao, B.; Li, B.; Ozaki, Y. *Langmuir* **2003**, *19*, 4285.

(4) (a) Haes, A. J.; Hall, W. P.; Chang, L.; Klein, W. L.; Van Duyne, R. P. *Nano Lett.* **2004**, *4*, 1029. (b) Zhao, J.; Zhang, X.; Youzon, C. R.; Haes, A. J.; Van Duyne, R. P. *Nanomedicine* **2006**, *1*, 219.

(5) (a) Sanders, A. W.; Routenberg, D. A.; Wiley, B. J.; Xia, Y.; Dufresne, E. R.; Reed, M. A. *Nano Lett.* **2006**, *6*, 1822. (b) Wiley, B.; Wang, Z.; Wei, J.; Yin, Y.; Cobden, D. H.; Xia, Y. *Nano Lett.* **2006**, *6*, 2273.

(6) Tao, A.; Sinsermsuksakul, P.; Yang, P. *Nat. Nanotechnol.* **2007**, *2*, 435.

(7) (a) Jin, R. C.; Cao, Y. W.; Mirkin, C. A.; Kelly, K. L.; Schatz, G. C.; Zheng, J. G. *Science* **2001**, *294*, 1901. (b) Jin, R. C.; Cao, Y. C.; Hao, E.; Metraux, G. S.; Schatz, G. C.; Mirkin, C. A. *Nature* **2003**, *425*, 487. (c) Xue, C.; Millstone, J. E.; Li, S.; Mirkin, C. A. *Angew. Chem., Int. Ed.* **2006**, *46*, 8436. (d) Zheng, X.; Xu, W.; Corredor, C.; Xu, S.; An, J.; Zhao, B.; Lombardi, J. R. *J. Phys. Chem. C* **2007**, *111*, 14962.

(8) (a) Sun, Y.; Mayers, B.; Xia, Y. *Nano Lett.* **2003**, *3*, 675. (b) Wiley, B. J.; Chen, Y.; McLellan, J.; Xiong, Y.; Li, Z. Y.; Ginger, D.; Xia, Y. *Nano Lett.* **2007**, *7*, 1032.

(9) (a) Ducamp-Sanguesa, C.; Herrera-Urbina, R.; Figlarz, M. *J. Solid State Chem.* **1992**, *100*, 272. (b) Sun, Y.; Yin, Y.; Mayers, B. T.; Herricks, T.; Xia, Y. *Chem. Mater.* **2002**, *14*, 4736. (c) Sun, Y.; Xia, Y. *Adv. Mater.* **2002**, *14*, 833.

(10) Wiley, B. J.; Chen, Y.; McLellan, J. M.; Xiong, Y.; Li, Z.-Y.; Ginger, D. S.; Xia, Y. *Nano Lett.* **2007**, *7*, 1032.

(11) (a) Pastoriza-Santos, I.; Liz-Marzan, L. M. *Nano Lett.* **2002**, *2*, 903. (b) Metraux, G. S.; Mirkin, C. A. *Angew. Chem., Int. Ed.* **2007**, *46*, 2036. (c) Sun, Y.; Xia, Y. *Adv. Mater.* **2003**, *15*, 695. (d) Bastys, V.; Pastoriza-Santos, I.; Rodríguez-González, B.; Vaisnoras, R.; Liz-Marzán, L. M. *Adv. Fun. Mater.* **2006**, *16*, 766. (e) Washio, I.; Xiong, Y.; Yin, Y.; Xia, Y. *Adv. Mater.* **2006**, *18*, 1745.

(12) (a) Germain, V.; Li, J.; Ingert, D.; Wang, Z.; Pileni, M. P. *J. Phys. Chem. B* **2003**, *107*, 8717. (b) Maillard, M.; Giorgio, S.; Pileni, M. P. *Adv. Mater.* **2002**, *14*, 1084. (c) Maillard, M.; Giorgio, S.; Pileni, M. P. *J. Phys. Chem. B* **2003**, *107*, 2466. (e) Hao, E.; Kelly, K. L.; Hupp, J. T.; Schatz, G. C. *J. Am. Chem. Soc.* **2002**, *124*, 15182. (f) Maillard, M.; Huang, P.; Brus, L. *Nano Lett.* **2003**, *3*, 1611. (g) Jiang, L.; Xu, S.; Zhu, J. M.; Zhang, J.; Zhu, J. J.; Chen, H. *Inorg. Chem.* **2004**, *43*, 5877.

(13) (a) Im, S. H.; Lee, Y. T.; Wiley, B.; Xia, Y. *Angew. Chem., Int. Ed.* **2005**, *44*, 2154. (b) Sun, Y.; Xia, Y. *Science* **2002**, *298*, 2176.

(14) (a) McLellan, J. M.; Siekkinen, A.; Chen, J.; Xia, Y. *Chem. Phys. Lett.* **2006**, *427*, 122. (b) Jiang, X.; Zeng, Q.; Yu, A. *Nanotechnology* **2006**, 174929. (c) Chen, S.; Fan, Z.; Carroll, D. L. *J. Phys. Chem. B,* **2002**, *106*, 10777.

(15) Chen, J.; McLellan, J. M.; Siekkinen, A.; Xiong, Y.; Li, Z.-Y.; Xia, Y. *J. Am. Chem. Soc.* **2006**, *128*, 14776.

(16) Chen, Y.; Wang, C.; Ma, Z.; Su, Z. *Nanotechnology* **2007**, *18*, 325602.

(17) Wiley, B.; Herricks, T.; Sun, Y.; Xia, Y. *Nano Lett.* **2004**, *4*, 1733.

(18) (a) Hildebrandt, P.; Stockburger, M. *J. Phys. Chem.* **1984**, *88*, 5935. (b) Wehling, B.; Hill, W.; Klockow, D. *J. Mol. Struct.* **1995**, *349*, 117. (c) Schneider, S.; Grau, H.; Halbig, P.; Freunscht, P.; Nickel, U. *J. Raman Spectrosc.* **1996**, *27*, 57. (d) Grochala, W.; Kudelski, A.; Bukowska, J. *J. Raman Spectrosc.* **1998**, *29*, 681.

(19) (a) Campbell, M.; Lecompte, S.; Smith, W. E. *J. Raman Spectrosc.* **1999**, *30*, 37. (b) Fu, S.; Zhang, P. *J. Raman Spectrosc.* **1992**, *23*, 93.

(20) An, J.; Tang, B.; Ning, X.; Zhou, J.; Xu, S.; Zhao, B.; Xu, W.; Corredor, C.; Lombardi, J. R. *J. Phys. Chem. C* **2007**, *111*, 18055.

(21) (a) Schatz, G. C.; Van Duyne, R. P. In *Handbook of Vibrational Spectroscopy*; Chalmers, J. M., Griffiths, P. R., Eds.; Wiley: New York, 2002. (b) Brioude, A.; Pileni, M. P. *J. Phys. Chem. B* **2005**, *109*, 23371.

(22) Wang, Z. L. *J. Phys. Chem. B* **2000**, *104*, 1153.

(23) Millstone, J. E.; Métraux, G. S.; Mirkin, C. A. *Adv. Funct. Mater.* **2006**, *16*, 1209.

(24) (a) Whitney, A. V.; Elam, J. W.; Zou, S.; Zinovev, A. V.; Stair, P. C.; Schatz, G. C.; Van Duyne, R. P. *J. Phys. Chem. B* **2005**, *109*, 20522. (b) Haes, A. J.; Hall, W. P.; Chang, L.; Klein, W. L.; Van Duyne, R. P. *Nano Lett.* **2004**, *6*, 1029.

(25) (a) McLellan, J. M.; Li, Z.; Siekkinen, A. R.; Xia, Y. *Nano Lett.* **2007**, *7*, 1013. (b) Lu, L.; Kobayashi, A.; Tawa, K.; Ozaki, Y. *Chem. Mater.* **2006**, *18*, 4894. (c) Zhang, J.; Li, X.; Sun, X.; Li, Y. *J. Phys. Chem. B* **2005**, *109*, 12544.

JP802694P